

Seismic response of bridge pier supported on rocking shallow foundation

Deviprasad B. S.* and Dodagoudar G. R.^a

Geotechnical Engineering Division, Department of Civil Engineering, Indian Institute of Technology Madras, Chennai - 600036, India

(Received September 20, 2019, Revised February 14, 2020, Accepted March 10, 2020)

Abstract. In the seismic design of bridges, formation of plastic hinges plays an important role in the dissipation of seismic energy. In the case of conventional fixed-base bridges, the plastic hinges are allowed to form in the superstructure alone. During seismic event, such bridges may be safe from collapse but the superstructure undergoes significant plastic deformations. As an alternative design approach, the plastic hinges are guided to form in the soil thereby utilizing the inevitable yielding of the soil. Rocking foundations work on this concept. The formation of plastic hinges in the soil reduces the load and displacement demands on the superstructure. This study aims at evaluating the seismic response of bridge pier supported on rocking shallow foundation. For this purpose, a BNWF model is implemented in OpenSees platform. The capability of the BNWF model to capture the SSI effects, nonlinear behavior and dynamic loading response are validated using the centrifuge and shake table test results. A comparative study is performed between the seismic response of the bridge pier supported on the rocking shallow foundation and conventional fixed-base foundation. Results of the study have established the beneficial effects of using the rocking shallow foundation for the seismic response analysis of the bridge piers.

Keywords: bridge pier; shallow foundation; fixed-base foundation; rocking shallow foundation; BNWF model; soil-structure interaction; OpenSees

1. Introduction

Bridges are vital infrastructure facilities in the form of passages over waterways or land barriers to aid transportation. They serve a variety of commuters and are built to last for several decades. The structures to be located in highly seismic areas should be designed to withstand the seismic forces and perform as intended throughout the design life. However, it is not economically feasible to design a structure completely earthquake resistant. In the conventional design of structures, the mechanism to dissipate seismic energy is allowed by incorporating inelastic deformation in select components of the structure while the foundation remains fixed. In case of ordinary fixed-base bridges, the inelastic deformations are expected to occur due to flexural plastic hinges developed near both ends of the piers (CALTRANS SDC 2010).

The lateral forces acting on the deck cause the bridge pier to rotate about the base. As the foundation is relatively fixed owing to broader base width, as in the fixed-base design, the bridge pier alone is forced to rotate. This causes the formation of a plastic hinge near the base of the pier. The inelastic deformation due to plastic hinge causes a considerable damage to the bridge and its components. The plastic hinges cause steel members and rebar to yield,

concrete to crack, buckling and elongation of braces, permanent displacements and reduced lateral strength (Herdrich 2015). When the shear capacity of the bridge pier is exceeded, it fails. The fixed-base bridges may be safe from collapse during a seismic event but, the plastic deformations experienced by the bridge hinder traffic flow and necessitate repair, partial or perhaps even complete demolition.

The current practice of seismic design of foundation (e.g., fixed-base design of bridge foundation), prohibits the mobilization of foundation strength and plastic hinging in the soil-foundation system. This also prohibits mobilization of bearing capacity, sliding, uplifting and passive and shear failure in the case of embedded foundation. Anastasopoulos *et al.* (2010) suggested that the above failure mechanisms can be used for seismic protection of structures. The factor of safety against each of the above failure modes may seem reasonable owing to the difficulty in inspection and retrofitting of substructure after a strong earthquake event. However, it may lead to conservative oversimplifications. Harden *et al.* (2006) highlighted the above fact in the case of strong geometric nonlinearities such as foundation uplift and sliding. Neglecting such nonlinearities may prohibit the use of nonlinear energy dissipating mechanisms in seismic protection of superstructure when the seismic ground motion exceeds the design limit. The soil-foundation plastic yielding under seismic excitation is not only unavoidable but also be beneficial (Paolucci 1997, Pecker 2003, Gajan *et al.* 2003, 2008, Kutter *et al.* 2006, Chatzigogos *et al.* 2009, Gerolymos *et al.* 2008, 2009). Therefore, as an alternative approach, the foundation may be allowed to rock during the seismic event so that the plastic hinging occurs not in the superstructure but in the soil beneath the foundation

*Corresponding author, Research Scholar
E-mail: deviprasad.bsg@gmail.com

^aResearch Scholar
E-mail: deviprasad.bsg@gmail.com

^bProfessor

(Anastasopoulos *et al.* 2010).

The observations during post-earthquakes as documented by researchers (e.g., Pender and Robertson 1988, Butcher *et al.* 1998, Ulusay *et al.* 2002, 1998, Toh *et al.* 2008) suggest that the shallow foundation located near to the fault-induced ground rupture has responded exceptionally well with minimal damage to the foundation and associated structures. This fact suggests that the code based prescriptive design requirements are too conservative. The conservativeness can be reduced by decreasing the width of spread footing, which will in turn, induce rocking behaviour to the entire soil-foundation-structural system. The bridges supported on rocking foundations may undergo large displacements but suffer less damage with the possibility of re-centering after the strong earthquake. Also compared to fixed base bridges, the bridges on rocking foundation are economical as they require smaller width for the spread foundations and lesser number of piles in the case of pile foundations (Antonellis 2015).

Seismic response of superstructure is greatly influenced by the nonlinear behaviour of the supporting foundation and the soil medium. The earthquake resistant design of structures (ERDS) requires a realistic modelling of the superstructure, foundation, subsoil and interactions between them. The modelling of nonlinear behaviour of the superstructure is well developed but a less attention is given to the soil-structure system as a whole. Even though the foundation is considered, the nonlinearity of the soil and soil-foundation interaction is seldom accounted. The consideration of nonlinear soil-structure interaction (SSI) effects during earthquake may provide a great deal of information about the response at the soil-foundation interface (e.g., Cakir 2014, Karabork *et al.* 2014, Jiang *et al.* 2018, Zhang *et al.* 2018). The interaction analysis includes a significant portion of the overall system flexibility. In the past, the soil-foundation interaction (SFI) was represented in terms of elastic impedance functions to describe stiffness and damping characteristics (e.g., Novak 1974, Dobry and Gazetas 1988, Gazetas 1991). The approaches based on impedance functions may not capture the nonlinear behaviour of the foundation, which includes temporary gap formation between the footing and soil, settlement, sliding and rocking of foundation and energy dissipation through hysteretic effects. For practical applications, the impedance functions can be represented using mechanistic springs and dashpots (e.g., Veletsos and Meek 1974, Wolf 1997, Wolf and Song 2002). The realistic representation of structural response requires improved tools to model the nonlinear SSI. Over the years, a few studies have been reported on modelling the behaviour of soil-foundation-structure systems using Winkler based approaches (e.g., Taylor *et al.* 1981, Chopra and Yim 1985, Paolucci and Pecker 1997, Allotey and El Naggar 2003, 2007, Harden *et al.* 2003, Raychowdhury 2008, Limkatanyu *et al.* 2012, Antonellis 2015, Lee *et al.* 2015, Hassan 2017, Mangalathu *et al.* 2017, Amini *et al.* 2018, Gonzalez *et al.* 2018, Jamil and Ahmad 2019, Mangalathu *et al.* 2019). One of the approaches is the beam on nonlinear Winkler foundation (BNWF) approach which consists of elastic beam-column elements to capture the structural footing behaviour and zero-length soil elements to model the soil-footing interaction.

The present study investigates the behavior of bridge pier supported on rocking shallow foundation using the BNWF model in OpenSees platform. The centrifuge test results of the shear wall on shallow foundation under slow cyclic loading are used to validate the capabilities of the BNWF model to capture the SSI effects and nonlinear behavior. The centrifuge test results of the dynamic loading are also used to check the suitability of the model under such loading conditions. The applicability of the BNWF model for seismic response analysis of the bridge pier supported on the rocking shallow foundation is examined by comparing the results of shake table tests. Finally, the response of the bridge pier is compared with the fixed-base foundation to establish the beneficial effects of using the rocking shallow foundation for the enhanced performance assessment of the bridge piers.

2. Theoretical consideration

2.1 Characteristics of rocking foundations

Fig. 1 shows the schematic of a shallow rocking foundation supporting a bridge pier. The total vertical load (Q) acting on the soil-foundation interface is due to deck mass (m_d), mass of the overburden soil (m_o) and the footing mass (m_f).

2.1.1 Critical contact area and critical contact length

The Q is equal to the limiting bearing capacity when the foundation strength is fully mobilized. The minimum bearing area to support the Q when the foundation strength is fully mobilized is called as critical contact area (A_c). The contact length between the soil and footing interface is called as critical contact length (L_c). At limiting condition, the limiting bearing capacity (q_{bl}) is equal to Q divided by the A_c . The q_{bl} is expressed as:

$$q_{bl} = \frac{Q}{L_f \times B_f} \quad (1)$$

The value of q_{bl} can be evaluated using the conventional bearing capacity equations. Iterations are required to solve for L_c because the L_c changes during a seismic event and hence the value of q_{bl} . The iterations will be stopped when the values of q_{bl} and L_c are satisfied the following equation:

$$L_c = \frac{Q}{q_{bl} \times B_f} \quad (2)$$

2.1.2 Rocking moment capacity

When the lateral seismic forces act on the foundation, the overturning moments are induced about the center of the base of the foundation. When the overturning moment becomes equal to the resisting moment capacity, the footing starts to rotate. The resisting rocking moment capacity of the footing is defined as (Gajan and Kutter 2008)

$$M_{c_foot} = \frac{Q \times L_f}{2} \left(1 - \frac{A_c}{A} \right) \quad (3)$$

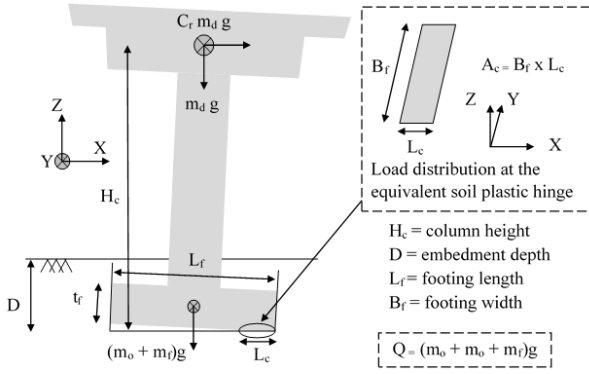


Fig. 1 Schematic of a rocking foundation

During a seismic event, as the foundation starts to rock, the contact area varies due to rocking and uplift of the foundation leading to variable values of $M_{c,foot}$. The contact area approaches A_c at the limiting condition. If the contact area is smaller than the A_c , the footing is likely to exhibit plunging failure (Deng *et al.* 2012). In general, the rocking behaviour is reported to be well defined and non-degrading during dynamic loading (Taylor *et al.* 1981, Gajan and Kutter 2008, Deng *et al.* 2012).

2.1.3 Hinging mechanism

The plastic hinges are formed in reinforced-concrete (RC) columns when the flexural capacity is exceeded. Similarly, in the case of rocking foundations, equivalent plastic soil hinges are formed when the overturning moment exceeds the resisting moment capacity. At limiting condition, the contact length between the soil and footing is L_c . If the contact length is smaller than L_c , the overturning moment exceeds the resisting moment capacity and the footing starts to rotate about L_c . In this case, the L_c represents the width of the equivalent soil plastic hinge (Fig. 1). The plastic hinge formed in RC columns and equivalent soil plastic hinge in the case of rocking foundations are conceptually similar, but the rocking foundations perform better owing to its ductile behaviour, re-centering characteristics, better energy dissipation mechanism and non-degrading moment capacity (Deng *et al.* 2012).

2.1.4 Base shear coefficient

In case of RC columns, the ratio of the lateral force to the superstructure weight required to mobilize the flexural bending moment capacity is defined as base shear coefficient. Similarly, the base shear coefficient (C_r) for rocking foundation is described as the lateral force required to mobilize the $M_{c,foot}$ and is expressed as (Deng *et al.* (2012).

$$C_r = \frac{L_f}{2 \times H_c} \left(1 - \frac{A_c}{A} \right) (1 + r_m) \quad (4)$$

where $r_m = (m_o + m_f)/m_d$ describes the stabilizing effect of m_o and m_f

2.2 BNWF model

The approach based on BNWF model consists of elastic

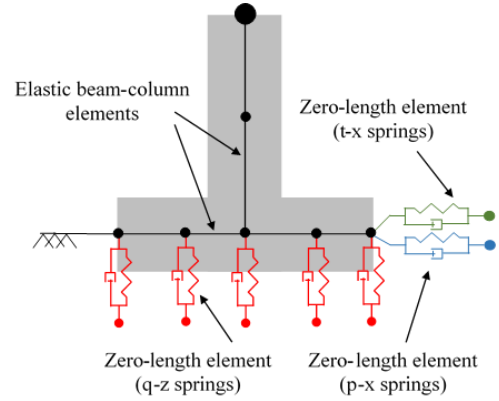


Fig. 2 Schematic of BNWF model for shallow foundation

beam-column elements and zero-length soil elements to capture the structural footing behaviour and to model the soil-footing interaction respectively. In the case of pile foundation, the nonlinear inelastic behaviour of the soil is represented using QzSimple1, PySimple1 and TzSimple1 material models available in the OpenSees (Boulanger *et al.* 1999, Boulanger 2000) whose backbone curves are calibrated with pile load tests. For shallow foundation, modified versions of the same are used which are calibrated with shallow foundation load tests (Raychowdhary 2008). Fig. 2 shows the schematic of the BNWF model for shallow foundation. The q-z, p-x and t-x springs simulate vertical load-displacement, horizontal passive load-displacement and shear-sliding behaviour respectively. A typical zero-length element used in the BNWF model is depicted in Fig. 3(a). The soil-foundation separation is taken into account in q-z and p-x springs using gap elements, added in series with the elastic and plastic components. The elastic component of the spring captures the far-field response while the plastic component captures the near-field response. The zero-length element springs are characterized by a nonlinear backbone curve resembling a bilinear behaviour with linear and nonlinear regions representing the degradation of the stiffness. A typical backbone curve for QzSimple1 material used in the BNWF model is shown in Fig. 3(b).

The equations to describe the behaviour of QzSimple1, PySimple1 and TzSimple1 are similar. Mathematically, QzSimple1 material model is expressed as (Raychowdhary 2008)

$$q = k_{in} z \quad (5)$$

The elastic region is defined by

$$q_0 = C_r q_{ult} \quad (6)$$

where k_{in} is the initial elastic tangent stiffness, q is the instantaneous load, z is the instantaneous displacement, q_0 is the load at yield point, and C_r is the parameter describing the extent of the elastic portion.

The nonlinear portion in the backbone curve is described by

$$q = q_{ult} - (q_{ult} - q_0) \left[\frac{C_r z_{50}}{C_r z_{50} + [z^p + z_0^p]} \right]^n \quad (7)$$

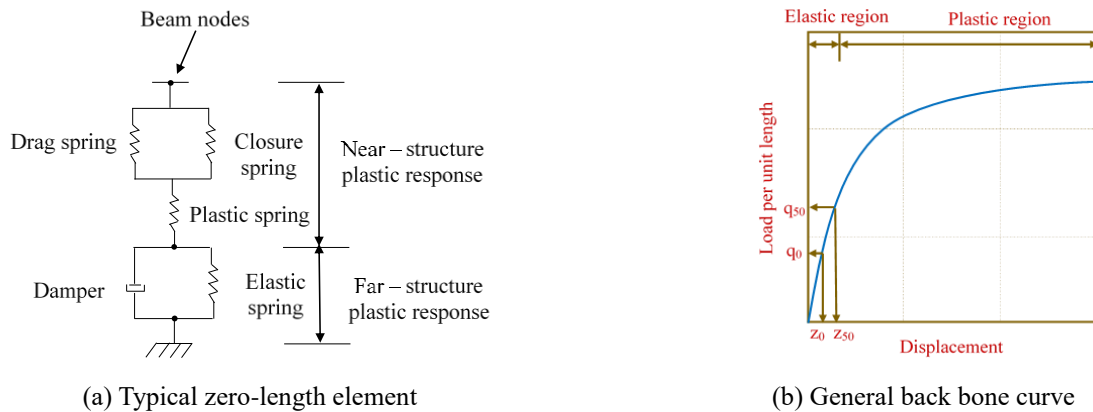


Fig. 3 Schematic of Zero-length element

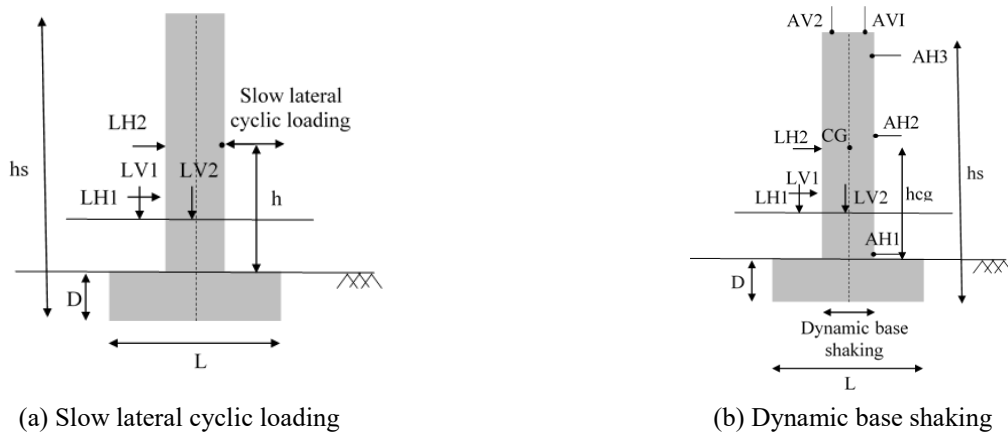


Fig. 4 Geometry and instrumentation used for the shear wall-footing in centrifuge experiments

where q_{ult} is the ultimate load, z_{50} is the displacement at 50% of the ultimate load, q_0 is the load at yield point, z_0 is the displacement at yield point and c and n are the parameters that describe the shape of the backbone curve post yield. The expressions for PySimple1 and TzSimple1 materials are similar to that of QzSimple1 material with corresponding variations in c , n and C_r parameters.

3. Finite element modelling

The efficacy of the BNWF model to incorporate the SSI effect is assessed by validating the results of the OpenSees analysis with that of the centrifuge test results from the literature. The centrifuge experiment pertains to shear wall on shallow foundation. In another case, the performance of the developed 2D FE model of the bridge pier supported on rocking foundation is studied by comparing the results of OpenSees simulations with that of the shake table test results. Validation of the BNWF model with the experimental data gives confidence in the OpenSees analysis.

3.1 Validation with centrifuge test results: Shear wall on a shallow foundation

Researchers at UC Davis, NEES facility carried out centrifuge experiments on shear wall structures with

shallow footing. Each experiment was involved in subjecting the shear wall-footing model to different loading conditions. In the present study, three centrifuge test results in which two are slow lateral cyclic loading cases and one is dynamic loading case are considered (Rosebrook and Kutter 2001, Gajan *et al.* 2003, Thomas *et al.* 2005). Fig. 4 shows the geometry, instrumentation and loading methods adopted in the centrifuge experiments.

The tests involved for the slow cyclic loading cases were performed under displacement control. The sinusoidal displacement histories were applied and the corresponding forces were measured using load cells attached to the actuator. In each set of experiment, two linear vertical potentiometers (LV1 and LV2) and two linear horizontal potentiometers (LH1 and LH2) attached to fixed locations were used to measure the displacements. The instrumentation for dynamic base shaking tests included two vertical and two horizontal potentiometers and three horizontal and two vertical accelerometers (AH1, AH2, AH3, AV1 and AV2) to measure the accelerations. The height of the shear wall is, $H = 10.1$ m. Table 1 shows the data of the centrifuge experiments and the same are used in the BNWF model. The factor of safety for static vertical loading (FS_v) is based on the weight of the structure and bearing capacity. Normalized moment to shear ratio is $M/(HL)$ in the case of dynamic loading, however for slow lateral cyclic tests, the same is taken as the normalized height of lateral loading (h/L).

Table 1 Data of shear wall-footing structure used in centrifuge tests*

Soil type	Test type	Mass (Mg)	L (m)	B (m)	D/B	FSv	M/(HL)
Sand, $D_r = 80\%$	Slow lateral cyclic	28	2.8	0.65	0	2.6	1.72
Clay, $C_u = 100$ kPa	Slow lateral cyclic	36	2.7	0.65	0	2.8	1.80
Sand, $D_r = 80\%$	Dynamic base shaking	36	2.8	0.65	0	4.0	1.80

*Rosebrook and Kutter (2001), Gajan *et al.* (2003), Thomas *et al.* (2005)

Table 2 BNWF model parameters for validation against centrifuge test results

Soil type	Test type	E (MPa)	ν	C_{rad} (%)	TP (%)	L_{end}/L (%)	R_k
Sand, $D_r = 80\%$	Slow lateral cyclic	45	0.35	5	10	10	2.5
Clay, $C_u = 100$ kPa	Slow lateral cyclic	40	0.4	5	10	10	2.5
Sand, $D_r = 80\%$	Dynamic base shaking	45	0.35	5	10	10	2.5

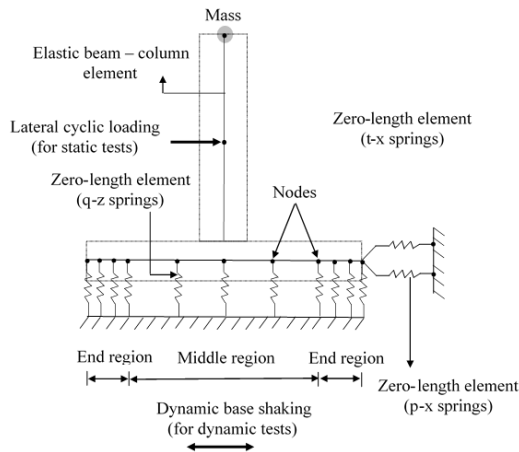
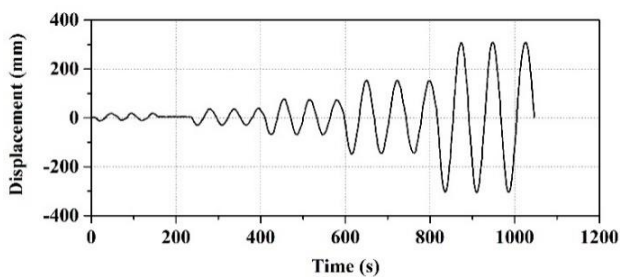
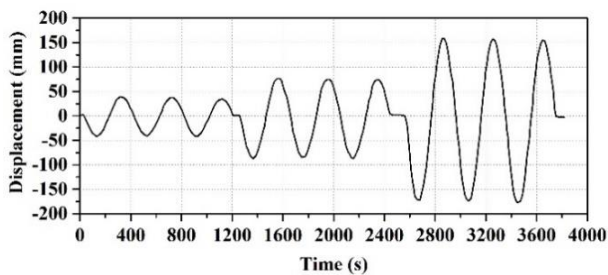


Fig. 5 Schematic of shear wall-footing in BNWF model

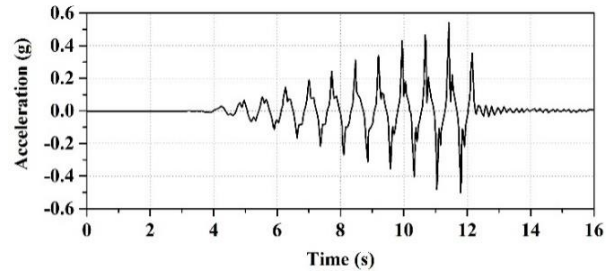


(a) Slow lateral cyclic test in sand



(b) Slow lateral cyclic test in clay

Fig. 6 Inputs used in OpenSees simulations



(c) Dynamic base shaking test in sand

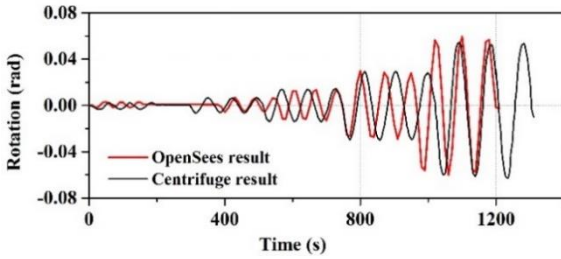
Fig. 6 Continued

The shear wall-footing system tested in the centrifuge is modelled using the BNWF model as shown in Fig. 5. The elastic beam-column element is used to model the shear wall and footing and zero-length elements are used to model the soil-footing interaction.

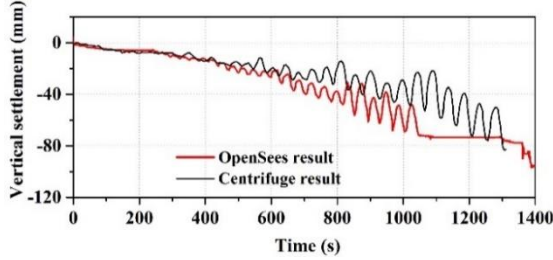
The q-z springs are attached to the bottom of the footing (Fig. 5). The distribution of these springs along the footing width enables the model to capture the moment-rotation behaviour. The ATC-40 (1996) suggests that the stiffer springs be placed at the end region to account for larger reaction developed at the end of the footing. The variable stiffness distribution along the footing width is modelled by keeping the spring spacing at closer intervals at the end regions and increasing the spacing at the middle region appropriately. The soil stiffness is calculated as per Gazetas (1991). The input parameters used in the finite element simulation are given in Table 2. The scale factor used in the centrifuge tests is 20. The finite element discretization considers the prototype dimensions using the above scale factor. The end length ratio (L_{end}/L), is the ratio of the length of end region to the total length of the footing. The vertical tension capacity (TP) is taken as 0-10% of the compression capacity. The stiffness intensity ratio (R_k), is the ratio of the end region stiffness to that of the mid region (FEMA-356 2000).

In OpenSees, the loading begins with the application of model self-weight in the vertical direction at the superstructure node under load control condition. Slow lateral cyclic loading is applied as displacement history at the superstructure node. Dynamic base shaking is applied as free-field accelerations at the base of the shear wall-footing model. The Newmark integrator and Newton algorithm are used to perform the nonlinear computations. The required response quantities, called as recorders in OpenSees, are set to monitor the forces, displacements and accelerations of the shear wall-footing model. Figs. 6(a) and 6(b) show the measured displacement time histories corresponding to the slow lateral cyclic tests performed in the centrifuge and the same are used as the inputs to the OpenSees model at the homologues points. Fig. 6(c) depicts the acceleration history used in the OpenSees, the same was used in the centrifuge test with scale factor.

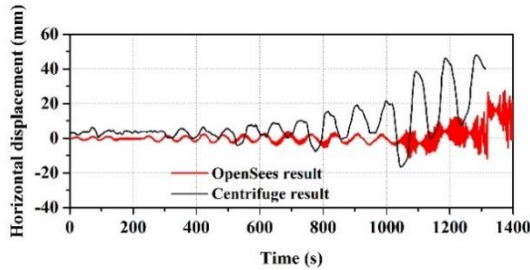
Figs. 7-10 compare the results of BNWF model (OpenSees simulation results) with the centrifuge test results. Figs. 7 and 8 pertain to slow cyclic tests performed in sand and clay respectively, whereas Fig. 9 pertains to the dynamic base shaking test. The response quantities



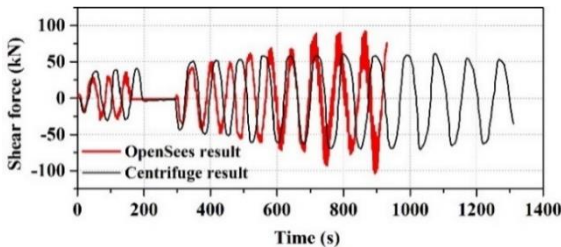
(a) Rotation of the footing



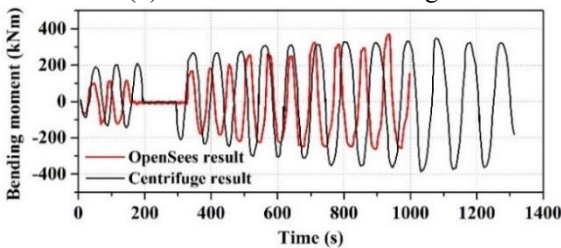
(b) Vertical settlement of the footing



(c) Horizontal displacement of the footing



(d) Shear force of the footing

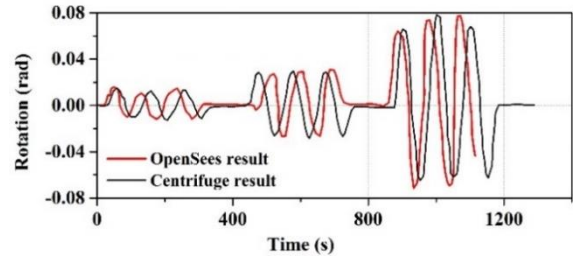


(e) Bending moment of the footing

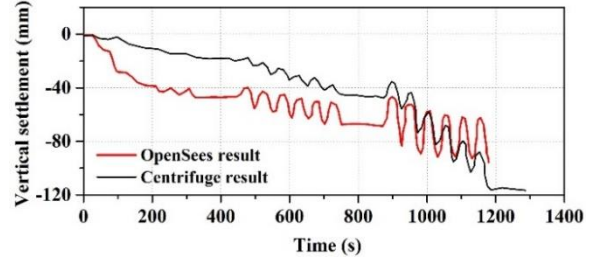
Fig. 7 Comparison of response recorded and obtained at the centre of the footing at base for slow lateral cyclic test in sand

presented are the rotation, vertical settlement, horizontal displacement, shear force, bending moment and settlement-rotation behaviour of the footing at the centre of the base.

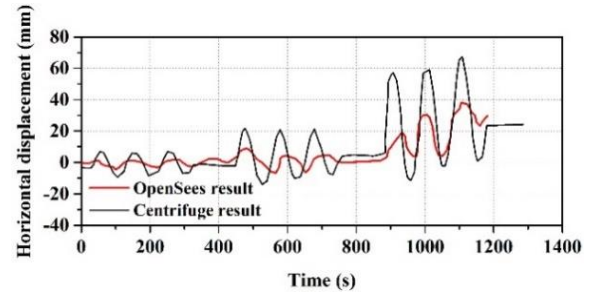
It is seen that the OpenSees results are in good agreement with the centrifuge results in terms of capturing the responses with regard to maximum moment, shear force, rotation and settlement. In the case of rotational behaviour,



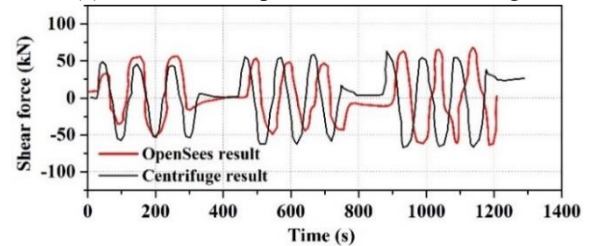
(a) Rotation of the footing



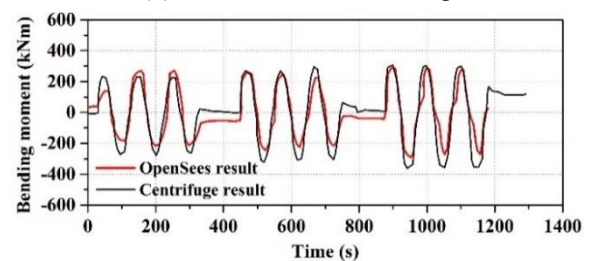
(b) Vertical settlement of the footing



(c) Horizontal displacement of the footing



(d) Shear force of the footing



(e) Bending moment of the footing

Fig. 8 Comparison of response recorded and obtained at the centre of the footing at base for slow lateral cyclic test on clay

error in the prediction of peak rotation of the footing by the BNWF model is less than 10% which is acceptable for practical purposes. The settlements are predicted reasonably well at lower amplitudes of the cyclic loading. At higher amplitudes, the BNWF model has over-predicted the settlement of the footing. However, the sliding and shear forces are under-predicted. This under-estimation is due to

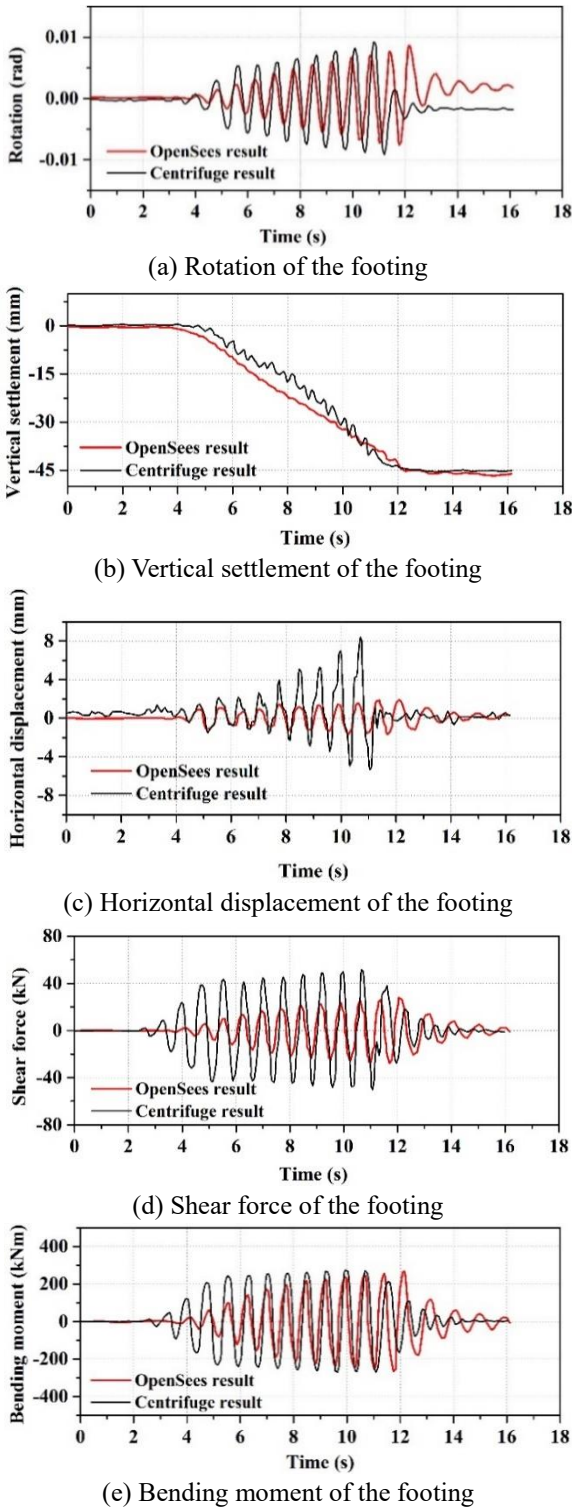


Fig. 9 Comparison of response recorded and obtained at the centre of the footing at base for dynamic base shaking test in sand

the lack of coupling between the lateral (t - x) and vertical (q - z) springs in the BNWF model. The maximum moment developed at the base of the footing is well predicted by the BNWF model. One of the most important design parameters of the foundation design is the permanent displacement after the earthquake event. The settlement-rotation behaviour of the footing confirms the expected

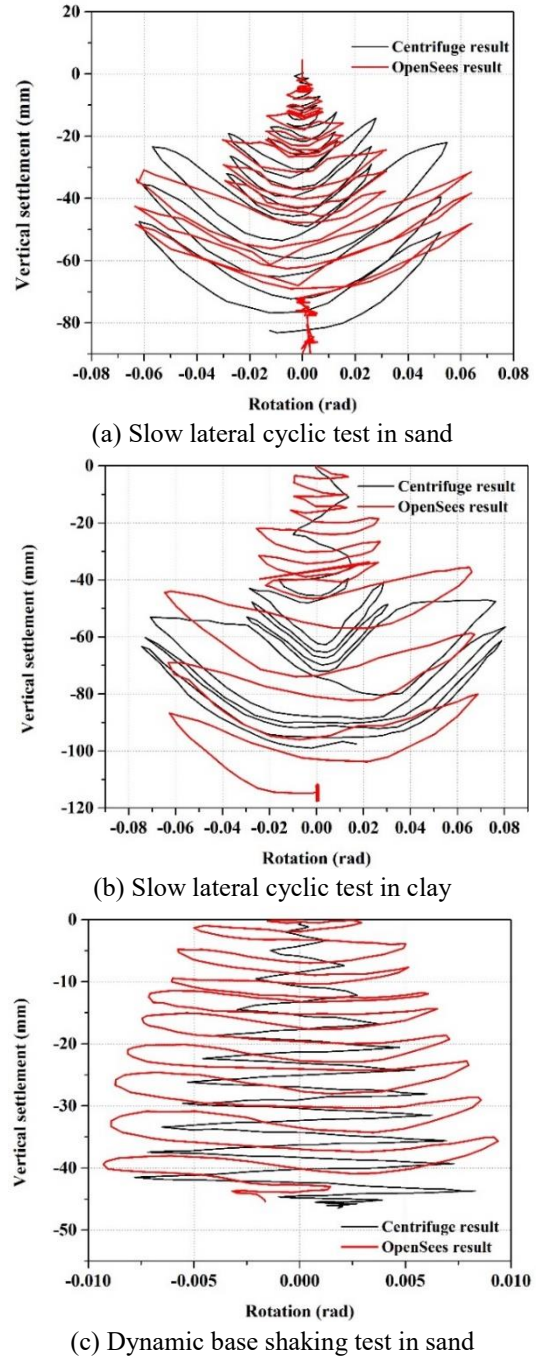


Fig. 10 Comparison of settlement-rotation behaviour of the footing at the center of the base

mechanism observed at the soil-footing interface. The settlement and uplift of the footing increase as the magnitude of rotation increases. It is seen that the settlement and rotation of the shear wall footing match well with the centrifuge results

3.2 Validation with shake table test results: Bridge pier on shallow foundation

If a numerical model is capable of realistically capturing the reversal of the deformation behaviour, then the model is good enough to be used for seismic response analysis. The

Table 3 Geometric and design parameters of pier-foundation system*

Soil type	Mass (Mg)	L (m)	B (m)	D/B	FSv	M/(HL)
Sand, $D_r = 85\%$	1200	7	1.4	0	3.6	1.9

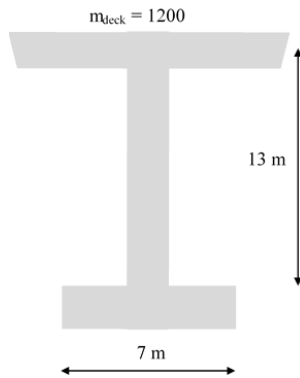
*Drosos *et al.* (2012)

Fig. 11 Schematic of bridge pier on shallow foundation used in shake table test

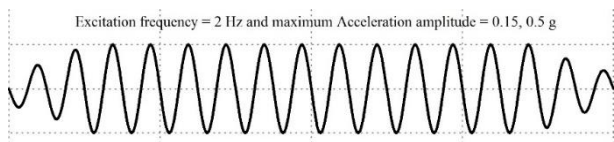


Fig. 12 Input acceleration time history used in OpenSees simulation

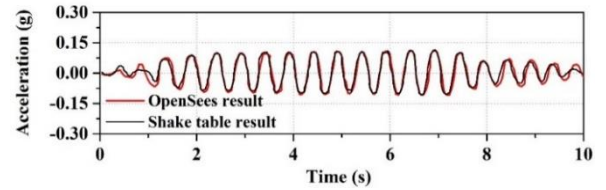
Table 4 BNWF model parameters for simulating shake table test

Soil type	Loading	E (MPa)	ν	C_{rad} (%)	TP (%)	L_{end}/L (%)	R_k
Sand, $D_r = 85\%$	Sinusoidal	45	0.35	5	10	16	2.5

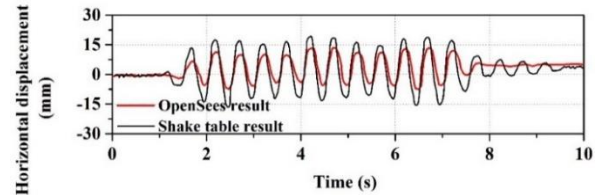
BNWF model used in the above section can be modified so that the seismic response analysis of the bridge pier supported on rocking shallow foundation could be performed.

The results of the OpenSees simulation are validated with the shake table test results. A series of reduced scale shake table tests were conducted at the Laboratory of Soil Mechanics of the National Technical University of Athens (NTUA), on the isolated bridge pier resting on surface foundation (Drosos *et al.* 2012, Anastasopoulos *et al.* 2013). The structural model was subjected to a variety of shaking events. The idealised prototype is a moderately tall RC bridge pier supported on the shallow foundation which in turn rests on the homogenous undrained soil stratum. The experimental model was deduced from the conceptual prototype with linear geometric scale of 1:20. Fig. 11 presents the idealised bridge pier on shallow foundation adopted for the shake table tests. Table 3 gives the geometric and design parameters of the prototype pier-foundation system

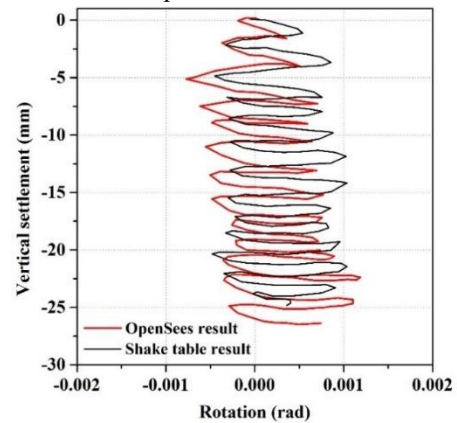
The structural model was tested under monotonic, slow cyclic and symmetric and non-symmetric seismic events. In the present study, the results of the shake table test performed using symmetric harmonic excitation are



(a) Acceleration at centre of base of the foundation



(b) Horizontal displacement at centre of the deck



(c) Settlement-rotation behaviour at centre of base of the foundation

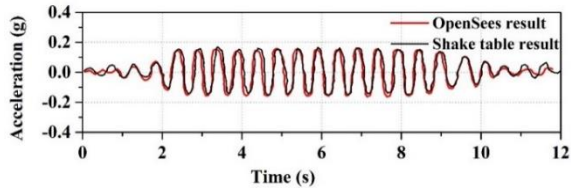
Fig. 13 Comparison of OpenSees and shake table results for $f_E = 2$ Hz and $A_E = 0.15$ g

only considered. Twelve cycles of the sinusoidal harmonic motion with 2 Hz excitation frequency (f_E) are used as the input motion. Two gradually increasing maximum acceleration amplitudes (A_E) of 0.15 and 0.5 g are considered for the OpenSees simulation. Table 4 gives the important BNWF model parameters used in the OpenSees simulation. Fig. 12 depicts the input motion used in the simulation

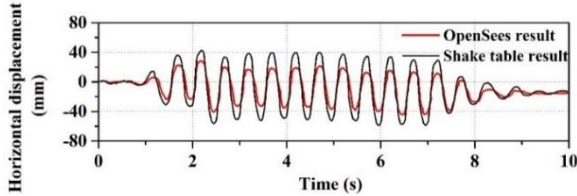
Figs. 13 and 14 compare the OpenSees results with that of the shake table for the bridge pier supported on shallow foundation. Fig. 13 pertains to the results of sinusoidal harmonic motion of $f_E = 2$ Hz and $A_E = 0.15$ g. Similarly, Fig. 14 depicts the results corresponding to sinusoidal harmonic motion of $f_E = 2$ Hz and $A_E = 0.5$ g. The responses evaluated are the acceleration and displacement time histories measured at the centre of the deck and settlement-rotation behaviour of the footing. It is noted that the OpenSees results are in good agreement with the shake table results.

3.3 Seismic response of bridge pier: Rocking isolation design and fixed-base design

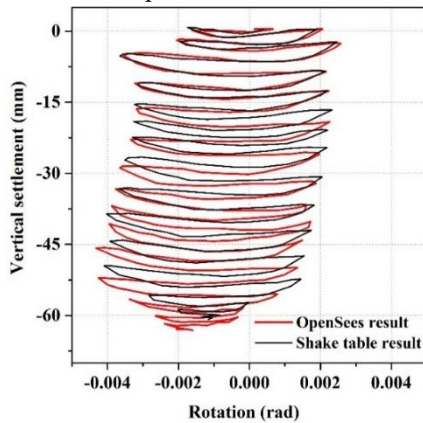
The bridge pier supported on shallow foundation, as shown in Fig. 11, is simulated using BNWF model in OpenSees. A comparative study is performed to highlight



(a) Acceleration at centre of base of the foundation



(b) Horizontal displacement at centre of the deck



(c) Settlement-rotation behaviour at centre of base of the foundation

Fig. 14 Comparison of OpenSees and shake table results for $f_E = 2$ Hz and $A_E = 0.5$ g

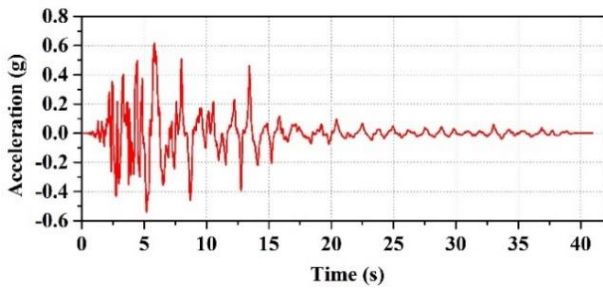


Fig. 15 Kobe 1995 earthquake, Takatori accelerogram

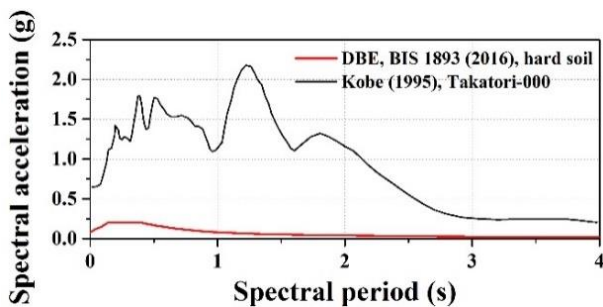


Fig. 16 Kobe earthquake response and IS design spectra

the effectiveness of the rocking foundation design approach over the conventional fixed-base design approach. In the

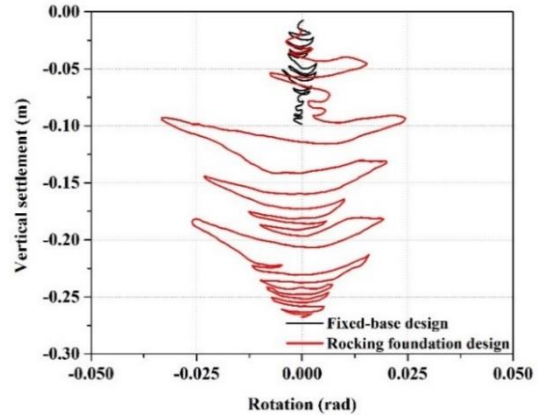


Fig. 17 Settlement-rotation behaviour of the bridge pier foundation system using two design approaches

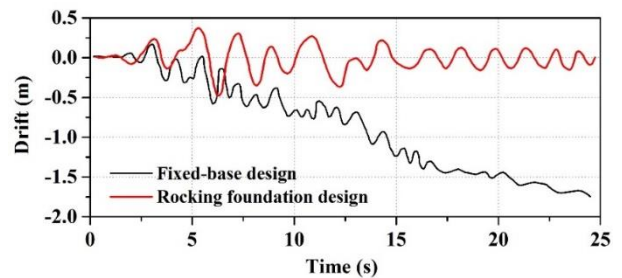


Fig. 18 Time histories of the drift of the deck at the centre

analysis, the geometrical and model parameters are kept same except the foundation width (B) and vertical factor of safety (FS_v). The B is taken as 14 m for the fixed-base design approach and for the bridge pier with rocking shallow foundation it is considered as 7 m. The width of 14 m for the foundation ensures that the foundation remains fixed. Further, the $FS_v = 5.4$ is considered for the fixed-base design approach and $FS_v = 2.7$ is used for the bridge pier with rocking shallow foundation. The higher FS_v values considered in the fixed-base design ensure that the soil does not yield and the plastic hinges will occur only in the superstructure. The 1995 Kobe earthquake, Takatori accelerogram (Fig. 15) is used as the input excitation at the center of the base of the BNWF model in the OpenSees simulation studies. The spectrum obtained corresponding to the Kobe earthquake input motion and the design basis earthquake (DBE) spectrum of IS: 1893(Part 1): 2016 are depicted in Fig. 16. It is seen that the Kobe earthquake spectrum is much higher than the IS spectrum and is capable of producing yield strains in the foundation medium. This helps in the formation of plastic hinge at the foundation level thereby introducing rocking foundation behaviour.

3.4 Results and discussion

Fig. 17 depicts the settlement-rotation behaviour of the fixed-base and rocking foundation design approaches. The conventionally designed fixed-base bridge pier has undergone smaller and limited amount of settlement. However, the bridge pier supported on rocking foundation experienced larger dynamic settlement. This is attributed to

the reduction in the contact area during rocking owing to the uplift of the foundation thereby increasing the stress because of the reduced bearing area of the foundation.

The time history of the horizontal displacement of the deck (drift) at the centre is depicted in Fig. 18 using the two design concepts. The horizontal displacement recorded here comprises of both the flexural distortion of the bridge pier and horizontal displacement due to rocking movement of the foundation. As seen from the figure that the bridge pier designed using fixed-base design concept shows larger values for the horizontal displacement. These displacements will definitely induce severe damage and even collapse of the bridge pier during seismic events. Provision of the wider foundation ($B = 14$ m) in the fixed-base design concept, in most of the cases, the foundation is going to behave as fixed one unlike in the case of rocking foundation. As the base is fixed, the plastic hinge will form in the bridge pier near to the base. Hence, most of the horizontal displacement is due to the flexural distortion of the bridge pier. Hence the bridge is expected to fail due to large plastic flexural distortion. Even if the bridge pier does not collapse, the plastic deformations experienced by the bridge pier necessitate repair or partial or perhaps even a complete demolition. On the other hand, the bridge pier supported on the rocking foundation ($B = 7$ m) experiences lesser residual horizontal displacement and the re-centering of the bridge pier is possible as seen in Fig. 18. The maximum horizontal displacement of the deck may be substantial but the residual values may be well within the tolerable limits after earthquake event. Under dynamic loading, the rocking movement will lead to possible re-centering of the foundation thereby providing adequate stability to the superstructure.

4. Conclusions

The OpenSees platform is used to model the SSI effects for the seismic behaviour of bridge pier supported on rocking shallow foundation using the BNWF model. The efficiency of the developed model is established by comparing the centrifuge results with that of the OpenSees. The results of the slow cyclic load tests on the sand and clay are used to compare the vertical settlement, rotation, horizontal displacement, shear force and bending moment at the centre of the base of the shear wall footing. The dynamic centrifuge results of the shear wall on shallow foundation in sand are also used to validate the developed BNWF model. The developed numerical model of the bridge pier supported on shallow foundation is also validated using shake table results. The loading cases considered for the validation are: $f_E = 2$ Hz and $A_E = 0.15g$ and $f_E = 2$ Hz and $A_E = 0.5g$. The acceleration, horizontal displacement and settlement-rotation behaviour of the bridge pier on shallow foundation are evaluated using OpenSees and compared with the shake table results. A comprehensive parametric study is performed to highlight the beneficial effects of the rocking foundation as a support to the bridge pier as opposed to the bridge pier designed with conventional fixed-base approach. Based on the results presented in the paper, the following conclusions are drawn:

- The developed numerical model using OpenSees for the bridge pier on rocking shallow foundation has a greater promise in the realistic assessment of the SSI effects. The responses evaluated by the OpenSees using the BNWF model are in good agreement with the shake table results. It is noted that the BNWF model can be used to represent the foundation and underlying soil as realistically as possible to capture the essential features of the SSI. Thus the present study has highlighted the applicability of the BNWF model for the seismic response analysis of the bridge piers supported on the rocking shallow foundation.
- The bridge pier supported on the rocking foundation shows better performance when compared to the bridge pier supported on fixed-base. The bridge pier designed with conventional fixed-base design would collapse owing to the excessive horizontal displacement of the deck or the bridge may undergo non-repairable structural damage requiring partial or even complete demolition. Moreover, the settlements in the case of rocking foundations are more but the bridge pier would survive owing to the possible re-centering after the earthquake. The reparability of the bridge pier supported on rocking foundation depends on the settlement tolerance.
- During extreme loading condition, if the collapse prevention and life safety are the design objectives, the rocking foundation will prove to be advantageous over the conventional fixed-base design. The results of the present study have demonstrated the effectiveness of using the rocking foundations in bridges for the enhanced performance. However, before advocating the adoption of rocking foundations in current bridge design codes, it is necessary to perform comprehensive deterministic and probabilistic performance analyses of bridge systems with rocking foundations.

References

- Allotey, N. and Naggar, M.H.E. (2003), "Analytical moment-rotation curves for rigid foundations based on a Winkler model", *Soil Dyn. Earthq. Eng.*, **23**(5), 367-381, [https://doi.org/10.1016/S0267-7261\(03\)00034-4](https://doi.org/10.1016/S0267-7261(03)00034-4).
- Allotey, N. and Naggar, M.H.E. (2007), "An investigation into the winkler modeling of the cyclic response of rigid footings", *Soil Dyn. Earthq. Eng.*, **28**(1), 44-57, <https://doi.org/10.1016/j.soildyn.2007.04.003>.
- Amini, F., Bitaraf, M., Eskandari Nasab, M. and Javidan, M. (2018), "Impacts of soil-structure interaction on the structural control of nonlinear systems using adaptive control approach", *Eng. Struct.*, **157**, 1-13. <https://doi.org/10.1016/j.engstruct.2017.11.071>.
- Anastasopoulos, I., Gazetas, G., Loli, M., Apostolou, M. and Gerolymos, N. (2010), "Soil failure can be used for seismic protection of structures", *Bull. Earthq. Eng.*, **8**(2), 309-326, <https://doi.org/10.1007/s10518-009-9145-2>.
- Anastasopoulos, I., Loli, M., Georgarakos, T. and Drosos, V. (2013), "Shaking table testing of rocking-isolated bridge pier on sand", *J. Earthq. Eng.*, **17**(1), 1-32, <https://doi.org/10.1080/13632469.2012.705225>.
- Antonellis, G., Gavras, A.G., Panagiotou, M., Kutter, B.L., Guerrini, G., Sander, A. and Fox, P.J. (2015), "Shake table test of large-scale bridge columns supported on rocking shallow foundations", *J. Geotech. Geoenviron. Eng.*, **141**(5), 04015009. [https://doi.org/10.1061/\(ASCE\)GT.1943-5606.0001284](https://doi.org/10.1061/(ASCE)GT.1943-5606.0001284).

- ATC 40 (1996), *Seismic Evaluation and Retrofit of Concrete Buildings*, Applied Technology Council, Redwood City, California, U.S.A.
- Boulanger, R.W. (2000), The PySimple1, QzSimple1, and TzSimple1 Material Documentation, Document for the OpenSees platform. <http://opensees.berkeley.edu>.
- Boulanger, R.W., Curras, C.J., Kutter, B.L., Wilson, D.W. and Abghari, A. (1999), "Seismic soil-pile-structure interaction experiments and analyses", *J. Geotech. Geoenviron. Eng.*, **125**(9), 750-759. [https://doi.org/10.1061/\(ASCE\)1090-0241\(1999\)125:9\(750\)](https://doi.org/10.1061/(ASCE)1090-0241(1999)125:9(750)).
- Butcher, G., Andrew, A. and Cleland, G. (1998), "The Edgcombe earthquake", Centre for Advanced Engineering, University of Canterbury, Christchurch, New Zealand.
- Cakir, T. (2014), "Backfill and subsoil interaction effects on seismic behaviour of a cantilever wall", *Geomech. Eng.*, **6**(2), 117-138, <http://doi.org/10.12989/gae.2014.6.2.117>.
- CALTRANS (2010). *Caltrans Seismic Design Criteria version 1.6*, California Department of Transportation, Sacramento, California, U.S.A.
- Chatzigogos, C., Pecker, A. and Salencon, J. (2009), "Displacement-based design of shallow foundations with macroelement", *Soils Found.*, **49**(6), 853-869. <https://doi.org/10.3208/sandf.49.853>.
- Chopra, A.K. and Yim S.C. (1985), "Simplified earthquake analysis of structures with foundation uplift", *J. Struct. Eng.*, **111**(4), 906-930. [https://doi.org/10.1061/\(ASCE\)0733-9445\(1985\)111:4\(906\)](https://doi.org/10.1061/(ASCE)0733-9445(1985)111:4(906)).
- Deng, L., Kutter, B.L. and Kunnath, S.K. (2012), "Centrifuge modeling of bridge systems designed for rocking foundations", *J. Geotech. Geoenviron. Eng.*, **138**(3), 335-344. [https://doi.org/10.1061/\(ASCE\)GT.1943-5606.0000605](https://doi.org/10.1061/(ASCE)GT.1943-5606.0000605).
- Dobry, R. and Gazetas, G. (1986), "Dynamic response of arbitrarily shaped foundations", *J. Geotech. Eng.*, **112**(2), 109-135. [https://doi.org/10.1061/\(ASCE\)0733-9410\(1986\)112:2\(109\)](https://doi.org/10.1061/(ASCE)0733-9410(1986)112:2(109)).
- Drosos, V., Georgarakos, T., Loli, M., Anastopoulos, I., Zarzouras, O. and Gazetas, G. (2012), "Soil-foundation-structure interaction with mobilization of bearing capacity: Experimental study on sand", *J. Geotech. Geoenviron. Eng.*, **138**(11), 1369-1386. [https://doi.org/10.1061/\(ASCE\)GT.1943-5606.0000705](https://doi.org/10.1061/(ASCE)GT.1943-5606.0000705).
- FEMA-356 (2000), *Prestressed and Commentary for the Seismic Rehabilitation of Buildings*, FEMA-356, Federal Emergency Management Agency, Washington, D.C., U.S.A.
- Gajan, S. and Kutter, B.L. (2008), "Numerical simulation of rocking behaviour of shallow footings and comparisons with experiments", *Proceedings of the BGA International Conference on Foundations*, Dundee, Scotland, June.
- Gajan, S., Phalen, J. and Kutter, B. (2003), "Soil-foundation structure interaction: shallow foundations. Centrifuge Data Report for the SSG02 Test Series" Data Report No. UCD/CGMDR-03/01, Center for Geotechnical Modeling, University of California, Davis, U.S.A.
- Gazetas, G. (1991), "Formulas and charts for impedances of surface and embedded foundations", *J. Geotech. Eng.*, **117**(9), 1363-1381. [https://doi.org/10.1061/\(ASCE\)0733-9410\(1991\)117:9\(1363\)](https://doi.org/10.1061/(ASCE)0733-9410(1991)117:9(1363)).
- Gerolymos, N., Giannakou, A., Anastopoulos, I. and Gazetas, G. (2008), "Evidence of beneficial role of inclined piles: Observations and summary of numerical analyses", *Bull. Earthq. Eng.*, **6**(4), 705-722. <https://doi.org/10.1007/s10518-008-9085-2>.
- Gonzalez, F., Padron, L., Carbonari, S., Morici, M., Aznarez, J., Dezi, F. and Leoni, G. (2018), "Seismic response of bridge piers on pile groups for different soil damping models and lumped parameter representations of the foundation", *Earthq. Eng. Struct. Dyn.*, **48**(3), 306-327, <https://doi.org/10.1002/eqe.3137>.
- Harden, C., Hutchinson, T. and Moore, M. (2006), "Investigation into the effects of foundation uplift on simplified seismic design procedures", *Earthq. Spectra*, **22**(3), 663-692.
- Hassan, A. (2017), "Winkler model for pile seismic analysis considering end constraints effects", *HBRC J.*, **14**(3), 316-320, <https://doi.org/10.1193/1.2217757>.
- Herdrich, B. (2015), "Parametric study of rocking shallow foundations under seismic excitation" M.Sc. Project Report, Portland State University, Portland, U.S.A.
- Jamil, I. and Ahmad, I. (2019), "Bending moments in raft of a piled raft system using Winkler analysis", *Geomech. Eng.*, **18**(1), 41-48, <http://doi.org/10.12989/gae.2019.18.1.041>.
- Jiang, S., Du, C. and Sun, L. (2018), "Numerical analysis of sheet pile wall structure considering soil-structure interaction", *Geomech. Eng.*, **16**(3), 309-320. <http://doi.org/10.12989/gae.2018.16.3.309>.
- Karabork, T., Deneme, I.O. and Bilgehan, R.P. (2014), "A comparison of the effect of SSI on base isolation systems and fixed-base structures for soft soil", *Geomech. Eng.*, **7**(1), 87-103, <http://doi.org/10.12989/gae.2014.7.1.087>.
- Kutter, B.L., Martin, G.R., Hutchinson, T., Harden, C., Gajan, S. and Phalen, J. (2006), "Workshop on modeling of nonlinear cyclic load-deformation behavior of shallow foundations", PEER workshop Report No. 2005/14, University of California Berkeley, U.S.A.
- Lee, J., Jeong, S. and Lee, J.K. (2015), "3D analytical method for mat foundations considering coupled soil springs", *Geomech. Eng.*, **8**(6), 845-850, <http://doi.org/10.12989/gae.2015.8.6.845>.
- Limkatanyu, S., Kwon, M., Prachasaree, W. and Chaiviriyawong, P. (2012), "Contact interface fiber section element: Shallow foundation modeling", *Geomech. Eng.*, **4**(3), 173-190. <http://doi.org/10.12989/gae.2012.4.3.173>.
- Mangalathu, S., Jeon, J.S. and Jiang, J.Q. (2019), Skew adjustment factors for fragilities of California box-girder bridges subjected to near-fault and far-field ground motions", *J. Bridge Eng.*, **24**(1), 04018109-1-13. [https://doi.org/10.1061/\(ASCE\)BE.1943-5592.0001338](https://doi.org/10.1061/(ASCE)BE.1943-5592.0001338).
- Mangalathu, S., Jeon, J.S. and DesRoches, R. (2017), "Critical uncertainty parameters influencing seismic performance of bridges using Lasso regression", *Earthq. Eng. Struct. Dyn.*, **47**(3), 784-801, <https://doi.org/10.1002/eqe.2991>.
- Novak, M. (1974), "Dynamic stiffness and damping of piles", *Can. Geotech. J.*, **11**(4), 574-598. <https://doi.org/10.1139/t74-059>.
- Paolucci, R. (1997), "Simplified evaluation of earthquake-induced permanent displacement of shallow foundations", *J. Earthq. Eng.*, **1**(3), 563-579. <https://doi.org/10.1080/13632469708962378>.
- Paolucci, R. and Pecker, A. (1997), "Seismic bearing capacity of shallow strip foundations on dry soils", *Soils Found.*, **37**(3), 95-105. https://doi.org/10.3208/sandf.37.3_95.
- Pecker, A. (2003), "Aseismic foundation design process, lessons learned from two major projects: the Vascode Gama and the Rion Antirion bridges", *ACI International Conference on Seismic Bridge Design and Retrofit*, University of California, San Diego, U.S.A.
- Pender, M.J. and Robertson, T.W. (1987), "Edgcombe earthquake: Reconnaissance report", *Bull. NZ Soc. Earthq. Eng.*, **20**(3), 201-249. <https://doi.org/10.1193/1.1585452>.
- Raychowdhury, P. (2008), "Nonlinear Winkler-based shallow foundation model for performance assessment of seismically loaded structures", Ph.D. Thesis, University of California, San Diego, California, U.S.A.
- Rosebrook, K.R. and Kutter, B.L. (2001), "Soil-foundation structure interaction: Shallow foundations. Centrifuge Data Report for the KRR03 Test Series", Data Report No.

- UCD/CGMDR-01/11, Center for Geotechnical Modeling, University of California, Davis, California, U.S.A.
- Taylor, P.W., Bartlett, P.E. and Weissing, P.R. (1981), "Foundation rocking under earthquake loading", *Proceedings of the 10th International Conference on Soil Mechanics and Foundation Engineering*, Stockholm, Sweden, June.
- Thomas, J.M., Gajan, S. and Kutter, B.L. (2005), "Soil-foundation structure interaction: Shallow foundations. Centrifuge Data Report for the SSG04 Test Series", Data Report No. UCD/CGMDR-05/02, Center for Geotechnical Modeling, University of California, Davis, California. U.S.A.
- Toh, J.C.W. and Pender, M.J. (2008), "Earthquake performance and permanent displacements of shallow foundations", *Proceedings of the 2008 New Zealand Society for Earthquake Engineering Conference*, Wairakei, New Zealand.
- Ulusay, R., Aydan, O. and Hamada, M. (2002), "The behaviour of structures built on active fault zones: Example from the recent earthquakes of Turkey", *Struct. Eng. Earthq. Eng.*, **19**(2), 149-167, <https://doi.org/10.2208/jscesee.19.149s>.
- Veletsos, A. and Meek, J. (1974), "Dynamic behaviour of building-foundation systems", *Earthq. Eng. Struct. Dyn.*, **3**(2), 121-138, <https://doi.org/10.1002/eqe.4290030203>.
- Wolf, J. (1997), "Spring-dashpot-mass models for foundation vibrations", *Earthq. Eng. Struct. Dyn.*, **26**(9), 931-949. [https://doi.org/10.1002/\(SICI\)1096-9845\(199709\)26:9<931::AID-EQE686>3.0.CO;2-M](https://doi.org/10.1002/(SICI)1096-9845(199709)26:9<931::AID-EQE686>3.0.CO;2-M).
- Wolf, J. and Song, C. (2002), "Some cornerstones of dynamic soil-structure interaction", *Eng. Struct.*, **24**(1), 13-28, [https://doi.org/10.1016/S0141-0296\(01\)00082-7](https://doi.org/10.1016/S0141-0296(01)00082-7).
- Zhang, J., Xie, Y. and Wu, G. (2018), "Seismic responses of bridges with rocking column-foundation: a dimensionless regression analysis", *Earthq. Eng. Struct. Dyn.*, **48**(1), 152-170, <https://doi.org/10.1002/eqe.3129>.